An Investigation of the Biosorption of Radioactive Gallium-67 in an Aqueous Solution Using Rose Residue

Hayrettin Eroglu,*,† Sinan Yapici,‡ and Erhan Varoglu†

Department of Nuclear Medicine, Ataturk University, 25240 Erzurum, Turkey, and Department of Chemical Engineering, Ataturk University, 25240 Erzurum, Turkey

This study investigates the adsorption of gallium-67, routinely used in nuclear medicine laboratories, in aqueous solution by using the waste of a rose-oil processing factory (rose residue). The experimental parameters were determined to be as follows: temperature, (10.0 to 40.0) °C; pH, (2.0 to 10.0); stirring speed, (300 to 720) rpm; particle size, (0.15 to 1.40) mm; and adsorbent dose, (1.0 to 15.0) $g \cdot L^{-1}$. It was seen that the most important parameters were pH, temperature, particle size, and adsorbent dose. The adsorption mechanism of the rose residue was examined by comparing the Fourier transform infrared (FTIR) spectra before and after adsorption. The ΔG and ΔH values were determined, and it was concluded that the absorption was endothermic and spontaneous. Absorption kinetics was studied, and it was observed that they fit a pseudo second-order model. As a result, it was found that the rose residue was a perfect absorbent for the adsorption of gallium-67.

1. Introduction

In nuclear medicine, diagnoses and treatments are determined using radioactive materials. In such practices, damaging wastes are produced because of both the radioactivity used in visualization or treatment and the unused radioactivity. It is indisputable that the radiation produced is detrimental to the environment. Indeed, the biological effects of radiation are very serious; there are no cells that are fully resistant to it. Radiation may obstruct the growth of the cell, perpetuate the growth of cells, cause chromosome breaks and abnormalities, and finally lead to the death of the cell. Furthermore, radiation may have destructive effects on the hematopoietic, lymphatic, reproductive, and gastrointestinal systems, as well as the skin, eyes, central nervous system, and other organs such as the heart, kidney, liver, and pancreas. It should be noted that these effects are lasting and serious.[1]

One of the radionuclides used for visualization purposes in nuclear medicine is ^{67}Ga, which is converted to its stable daughter product of ^{67}Zn via the following radioactive reaction:[2]

$$^{67}\mathrm{Ga} \rightarrow {}^{67}\mathrm{Zn} + \gamma^{-2}\cdot 93\ \mathrm{keV}\ (38\ \%) + \gamma^{-3}\cdot 185\ \mathrm{keV}\ (24\ \%) + \gamma^{-5}\cdot 300\ \mathrm{keV}\ (16\ \%) + \gamma^{-6}\cdot 394\ \mathrm{keV} \quad (t_{1/2} = 78.25\ \mathrm{h}) \quad (1)$$

The wastes of radioactive materials used in nuclear medicine affect the environment in several ways, and these effects can be seen, for example, in patients' urine. The safety measures currently practiced for decreasing risk are to keep liquid wastes in a waste tank and solid wastes in lead rooms until their radioactivity levels are low enough to discharge them into the environment. These methods are expensive and accomplish little with regard to minimizing the damage caused by radioactive materials. The lead rooms and waste tanks occupy large physical spaces, do not provide complete insulation, and are a waste of time and money. As a result, radioactive elements have to be deposited to the environment by dilution. This gives rise to radioactive pollution. Since the radioactive elements can turn into stable metals, they may cause metal pollution and even metal poisoning. Indeed, when radioactive elements mix with ground waters, they can seriously harm the environment.

Both global warming and population growth have exponentially increased the need for fresh water. As the use of nuclear energy becomes more commonplace, it becomes necessary to properly dispose of the harmful materials after use. Physicochemical methods such as reverse osmosis, ion exchange, precipitation, and lime coagulation, which are used to remove toxic metals from waste waters, are very expensive and inefficient for low concentrations.[3] Moreover, as a result of these operations, a significant amount of toxic substances still pollute the environment. However, biosorption is a possible alternative to these methods.[4] Microorganisms such as fungi, yeasts, bacteria, and marine organisms can absorb cationic and anionic materials in a liquid environment.[5−8] Again, using ion exchange, the aim is to remove radioactive materials. Indeed, the Amberlite ion exchanger resin has been used to remove iodine-131, which is an element used in nuclear medicine.[9] Koshima has examined the adsorption of thallium(III), gallium(III), gold(III), and iron(III) from hydrochloric acid solution using Amberlite XAD and Chelox100 resins, publishing his findings in a 1986 article.[10] Similarly, in research done on Cr-51 wastes, adsorption was accomplished using water plants such as *Eichornia crassipes*, *Pistia sp*., *Nymphaea alba*, *Mentha aquatic*, *Euphorbia sp.*, and *Lemna minor*.[11] It has been put forth in several studies that active carbon absorbs radioactive materials. Indeed, Kütahyalı (2002) used active carbon to remove uranium,[12] while Sinha et al. applied the method to remove radioactive iodine.[13]

To remove radionuclides, biosorbents with different characteristics are currently being used. This study is aimed to remove the ^{67}Ga radionuclide from aqueous media by using the waste of a rose-oil processing factory (rose residue). Thence, the solid

* Corresponding author. E-mail: heroglu@atauni.edu.tr. Tel.: +90 442 231 4553. Fax: +90 442 231 4544.
† Department of Nuclear Medicine.
‡ Department of Chemical Engineering.

10.1021/je901015a
Published on Web 06/11/2010

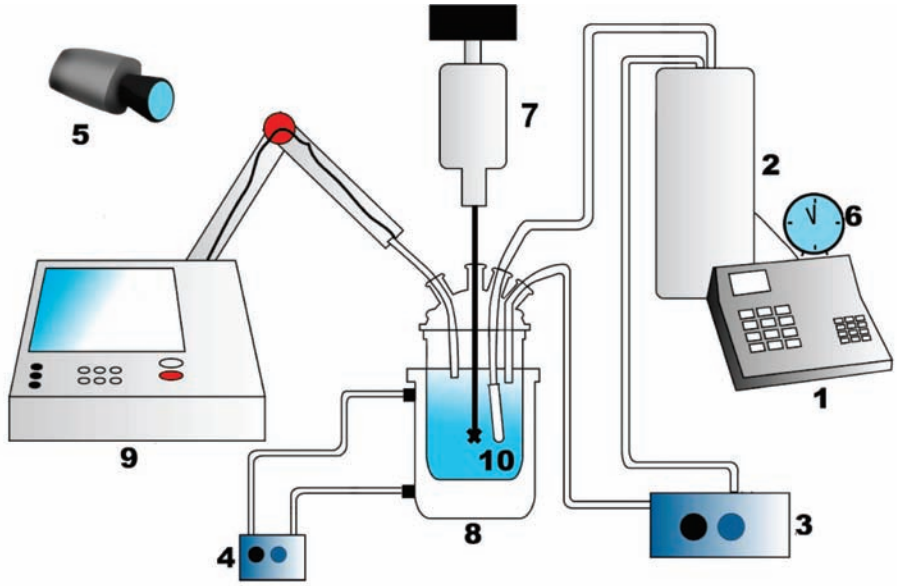

1.Radioactivity dosimeter	4. Circulating bath	7. Mechanical stirrer
2.Radioactivity reading chamber	5. Video camera	8.Jacketed adsorption vessel
3. Pump	6. Clock	9. pH meter
		10.Filter

Figure 1. Experimental system.[14]

waste from a rose oil plant will be employed for removing the other waste of nuclear medicine.

2. Materials and Methods

2.1. Adsorbent. The rose residue used in this study was supplied by the Sebat Ticaret Rose Attar Factory in Isparta, Turkey. Prior to its use in our experiments, the rose residue was washed with distilled water to remove any impurities. The decolorized and cleaned rose residue was dried at room temperature for a few days. It was then grinded with a strong grinder and sieved to a particle size of (0.150 to 0.212) mm. The Brunauer−Emmett−Teller (BET) surface area, bulk density, and zeta potential (at pH 2) of the biosorbent were determined to be 0.923 $m^2 \cdot g^{-1}$, 76 $g \cdot L^{-1}$, and −26.2 mV, respectively.

2.2. Experimental System. ^{67}Ga, which is one of the radioactive materials commonly used in nuclear medicine, was selected as the material to be adsorbed in the experiments. It must be remembered that since not only the radioactive state but also the stable product of this material is a metal, its adsorption also has importance. In the adsorption studies, the pH of the material was adjusted by adding 500 mL of pure water in a reactor. The temperature of the medium was kept constant at the desired level by connecting the reactor to a pump capable of adjusting the temperature, the solution was continuously stirred with a mixer, and to determine how much adsorption occurred, a dosimeter that measures radiation was used. A master flex pump was used to circulate the aqueous solution, and the radiation of the amount of the solution circulated was then measured. In this manner, the amount of radioactive material adsorbed was determined. Mixing of the solid adsorbent with the solution was avoided using a filter that did not adsorb the radioactive substance. The filter is placed immediately at the outlet of the solution from the vessel. All of the necessary steps were taken for an accurate measurement with the dosimeter. To minimize the involvement of the researcher with the radioactive medium, the experimental readings on digital screens were recorded by a video camera. The experimental system can be seen in Figure 1.[14] The experimental parameters were temperature, pH, stirring speed, adsorbent dose, and particle size. The following values were applied: pH, 2; temperature, 20 °C; adsorbent dose, 10 $g \cdot L^{-1}$; stirring speed, 600 rpm; and particle size, (0.150 to 0.212) mm.

2.3. Preparation of the Radioactive Solution. A solution which was 99 % radionuclide pure (^{67}Ga) and had a specific activity of 370 MBq$\cdot\mu g^{-1}$ on the calibration date was used to prepare the radioactive solution by taking into consideration the production date and the half time period. To obtain a 500 mL solution with an initial radionuclide concentration of approximately 18.5 MBq, which is similar to the average radioactive value of aqueous waste, this solution was added into the aqueous medium at an adjusted temperature, stirring speed, particle size, adsorbent dose, and initial pH value.

3. Results and Discussion

The removal of ^{67}Ga from the aqueous solution was carried out with rose residue. As it turned into steady state after 120 min, the values were calculated by taking the time elapsed into account and then evaluated. The parameters that affected the adsorption were examined in glass reactors under certain conditions. The results are discussed in the subsequent sections.

3.1. Effect of pH. The initial pH values for the adsorption of ^{67}Ga on the rose residue were 2.0, 4.0, 6.0, 7.0, 8.0, and 10.0. The removal of ^{67}Ga at different pH values is shown in Figure 3-a.

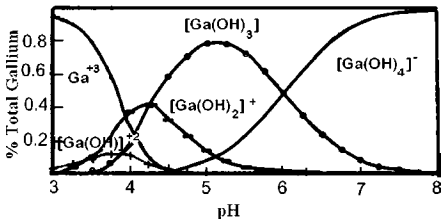

Figure 2. Change of chemical structure of gallium hydroxide with pH.[15]

The highest removal capacity was observed at pH 2, where 87.1 % of ^{67}Ga was adsorbed in 120 min. However, in the same circumstances, 71.3 % and 62 % of ^{67}Ga was adsorbed at pH = 4.0 and pH = 6.0, respectively (Figure 3a). No adsorption was observed at other pH values.

Ga is hydrolyzed very quickly in water. The chemical equations relating to the hydrolysis of Ga in water are given as follows:

$$[Ga]^{3+} + H_2O = [Ga(OH)]^{2+} + H^+ \quad (2)$$

$$[Ga(OH)]^{2+} + H_2O = [Ga(OH)_2]^+ + H^+ \quad (3)$$

$$[Ga(OH)_2]^+ + H_2O = [Ga(OH)_3] + H^+ \quad (4)$$

$$[Ga(OH)_3] + H_2O = [Ga(OH)_4]^- + H^+ \quad (5)$$

Gallium reactions with OH^- at different pH values are seen in Figure 2. Free gallium ions occur most frequently at pH 2. As can be seen from Figure 2, free gallium ions turned into $Ga(OH)_3$ and $[Ga(OH)_4]^-$ as values rose to pH 10.[15] The zeta potential value at pH 2 was calculated as −26.2 mV using a zeta meter 3.0. Free Ga^{3+} ions at pH 2 were adsorbed by interacting with the negatively charged adsorbent surface. They did not interact with the adsorbent surface at other pH values since their charge became neutral due to the reaction with OH^-. At pH 10 and above, negatively charged $[Ga(OH)_4]^-$ was not absorbed since two negatively charged particles, the gallium complex and the biosorbent, repel each other (the zeta potential value of the particle surface is −63.2 mV for pH = 10).

The best adsorption was observed at pH 2. For this reason, a pH value of 2 was accepted as the fixed condition for other experiments.

3.2. Effect of the Stirring Speed. During the adsorption of ^{67}Ga with the rose residue, stirring speeds were set at (360, 480, 600, and 720) rpm. The removal capacity of ^{67}Ga at different stirring speeds is shown in Figure 3b.

The highest removal capacity was observed at 720 rpm. It can be seen in Figure 3b that, at 720 rpm, 94.4 % of ^{67}Ga was adsorbed in 120 min, while under the same conditions at 320 rpm, only 84.4 % of ^{67}Ga was removed. As the stirring speed was increased, the Ga ions in the liquid reached the solid particles more easily. The reason for this is due to the decrease of a liquid film layer, resistance around solid surface as a result of the increase in stirring speed. However, significant changes were not observed when the results were compared. Experiments were carried out at 600 rpm because the particles were observed to scatter homogeneously without precipitation. We also considered the fact that higher speeds would make the process less energy-efficient.

3.3. Effect of Particle Size. In this study, the rose residue particle sizes used were (1.40 to 0.71) mm, (0.71 to 0.355) mm, (0.355 to 0.212) mm, and (0.212 to 0.150) mm. The removal of ^{67}Ga at different particle sizes is shown in Figure 3c.

It was observed that the highest removal capacity was at a particle size of (0.212 to 0.150) mm. It can be seen in Figure 3c that, at this particle size, 87.1 % of ^{67}Ga was adsorbed in 120 min, while under the same conditions at a particle size of (1.40 to 0.71) mm, only 67.5 % of ^{67}Ga was adsorbed. As expected, the output increased as the surface area increased.

3.4. Effect of Temperature. The adsorption of ^{67}Ga was examined at varying temperatures of (10, 20, 30, and 40) °C. The removal capacity of ^{67}Ga at different temperatures is shown in Figure 3d.

It was observed that the highest removal capacity occurred at 40 °C. It can be seen in Figure 3d that while 96.6 % of ^{67}Ga was adsorbed at 40 °C in 120 min, only 84.3 % of ^{67}Ga was adsorbed under the same conditions at 10 °C.

The effect of temperature is one of the important parameters. This indicates that the adsorption is a chemical and endothermic process because the output increases as the temperature rises.

3.5. Effect of Adsorbent Dose. In ^{67}Ga adsorption with the rose residue, (1, 2.5, 5, 10, and 15) g of solid rose residue was used for 1 L of liquid as adsorbent dose, and adsorption experiments were done at (10, 20, 30, and 40) °C. To obtain adsorption isotherms, the relationship between the adsorbent and the material adsorbed was observed at four different temperatures. The change in the ^{67}Ga removal capacity at the different temperatures and adsorbent doses is shown in Figure 3e. According to these values, it was concluded that, as the adsorbent dose increased, so did the efficiency of the adsorption. This situation can be explained by an increase in the number of active areas that absorb ^{67}Ga. All of the plots for different temperatures showed similar behavior; increasing the dose increased the biosorption percentage. The maximum biosorption yield was obtained at 15 $g \cdot L^{-1}$ and 40 °C. At equilibrium, an increase in the temperature from (10 to 40) °C increased the biosorption percentage from (34.5 to 50.2) % at an adsorbent dose of 1.0 $g \cdot L^{-1}$ and from 89 % to 99.6 % at a dose of 15.0 $g \cdot L^{-1}$.

3.6. Adsorption Isotherms. The purpose of adsorption isotherms is to provide a relationship at equilibrium between the adsorbed amount and the unabsorbed amount in the fluid bulk for a given temperature. There are many different adsorption isotherms. Among these, the models that best corresponded to the aims of the study were determined. Comments relating to these models are given below.

The Freundlich, Halsey, Hendersen, and Smith isotherms are convenient for multilayered adsorption. These isotherms show that there are active sites with heterogeneous energy distributions. Consistency with these isotherms is observed especially in heteroporous solids.[16−19] The results regarding these isotherms are presented in Table 1. In Table 1, K is a constant related to adsorption capacity ($L \cdot g^{-1}$), C is the concentration of the adsorbate in the solution at equilibrium ($mg \cdot L^{-1}$), q is the adsorbed amount per amount of adsorbent at equilibrium ($mg \cdot g^{-1}$), R^2 is the regression coefficient, n is a constant related to adsorption intensity, and W and W_b are constant parameters for the Smith model.

The statistical analysis showed that the isotherm data for the present work fit well with the isotherm models of Freundlich, Halsey, Henderson, and Smith. This is an indication that the active sites on the biosorbent surface had heterogeneous structures that consisted of adsorption sites of various species and that the adsorption process is a multilayered one.

According to the results, it is understood that the adsorption process has a multilayered, heterogeneous structure. For example, the fits of the equilibrium data of the Halsey and Smith isotherms are shown in Figure 4.

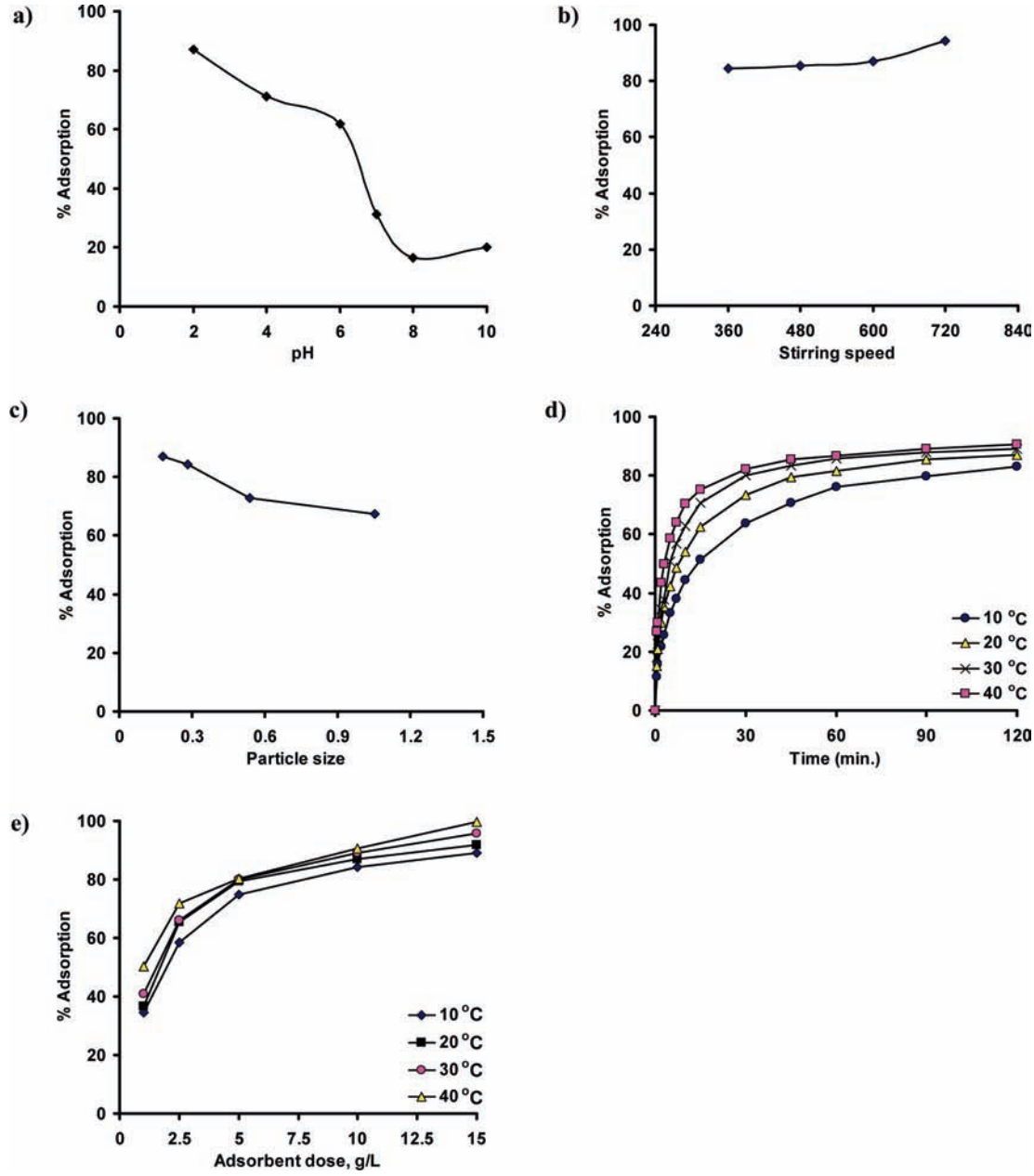

Figure 3. Effect of experimental parameters on adsorption. (a) Effect of initial pH values on adsorption of ^{67}Ga. (b) Effect of stirring speeds on adsorption of ^{67}Ga. (c) Effect of particle size on adsorption of ^{67}Ga. (d) Effect of temperature on the adsorption of ^{67}Ga. (e) Effect of adsorbent doses on adsorption of ^{67}Ga at different temperatures.

Table 1. Model Constants and Regression Coefficients of Isotherm Models

temperature, °C	10	20	30	40
isotherm and model equation	constants and regression coefficients			
Freundlich: $q = KC^{(1/n)}$ (2)	$n = 1.004$ $K = 0.531$ $R^2 = 0.9946$	$n = 1.092$ $K = 0.284$ $R^2 = 0.9839$	$n = 1.384$ $K = 0.0421$ $R^2 = 0.9511$	$n = 2.782$ $K = 0.00105$ $R^2 = 0.715$
Halsey: $\ln q = [(1/n) \ln K] - (1/n) \ln[\ln(1/C)]$ (3)	$n = 0.0959$ $K = 3.62$ $R^2 = 0.9912$	$n = 0.103$ $K = 3.42$ $R^2 = 0.9777$	$n = 0.125$ $K = 2.722$ $R^2 = 0.9608$	$n = 0.219$ $K = 1.028$ $R^2 = 0.7576$
Henderson: $\ln q = (1/n) \ln[-\ln(1 - C)] - (1/n) \ln K$ (4)	$n = 1.004$ $K = 1.89$ $R^2 = 0.9946$	$n = 1.092$ $K = 3.954$ $R^2 = 0.9839$	$n = 1.384$ $K = 80.17$ $R^2 = 0.9511$	$n = 2.782$ $K = 1.9444 \cdot 10^8$ $R^2 = 0.715$
Smith: $q = W_b - W \ln(1 - C)$ (5)	$W = 0.525$ $W_b = 8 \cdot 10^{-7}$ $R^2 = 0.9942$	$W = 0.5615$ $W_b = 3 \cdot 10^{-6}$ $R^2 = 0.9701$	$W = 0.636$ $W_b = 3 \cdot 10^{-6}$ $R^2 = 0.9926$	$W = 0.9199$ $W_b = 2 \cdot 10^{-6}$ $R^2 = 0.9633$

3.7. Thermodynamic Analysis. Thermodynamic parameters must be examined to be able to comment about whether adsorption is a physical or chemical process. Likewise, a discussion of thermodynamic parameters will allow us to determine the processes exothermic or endothermic character. Besides, whether or not adsorption will take place spontaneously can be decided by looking at the ΔG values.

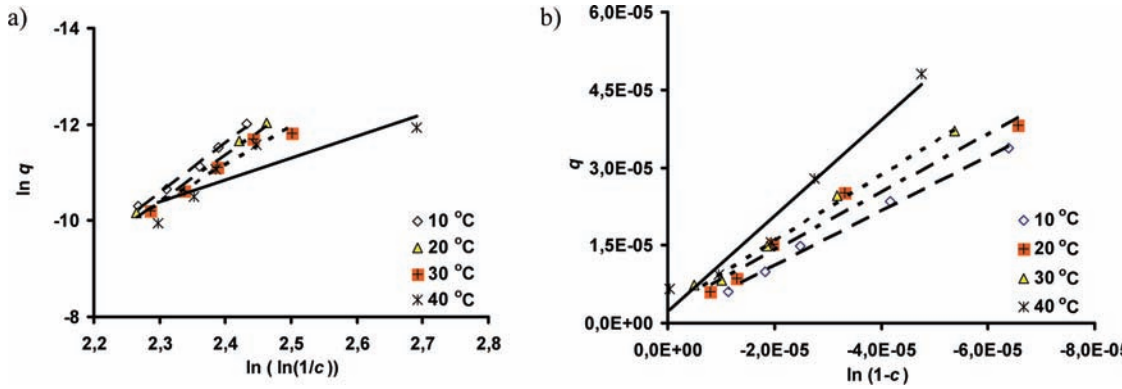

Figure 4. (a) Fit of data to the Halsey model. (b) Fit of data to the Smith model.

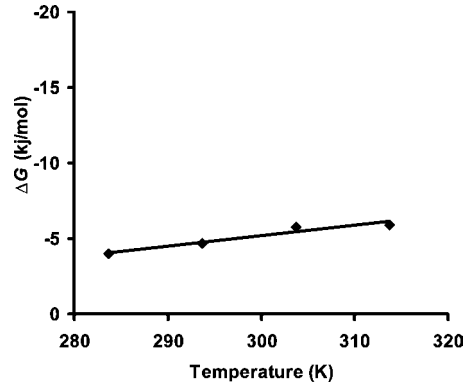

Figure 5. Plot of ΔG versus T.

Table 2. Values of ΔG at Different Temperatures

temperature, K	283	293	303	313
ΔG, J·mol^{-1}	−3963	−4674.4	−5746	−5908

Distribution coefficients can be calculated as follows:

$$k_D = C_{ads}/C_{notads} \quad (6)$$

From this, ΔG values are calculated by the following equation:

$$\Delta G = -RT \ln k_D \quad (7)$$

We should also consider the following:

$$\Delta G = \Delta H - T\Delta S \quad (8)$$

where k_D is the distribution coefficient, ΔG is the Gibbs free energy change (J·mol^{-1}), ΔH is the enthalpy change (J·mol^{-1}), R is the universal gas constant (8.314 J·K^{-1}·mol^{-1}), ΔS is the entropy change (J·mol^{-1}·K^{-1}), and T is the absolute temperature in kelvin (K).

ΔG can be calculated by eq 7 using the k_D values obtained from eq 6. The plot of ΔG versus T should give a straight line, as shown in Figure 5. When the graph of ΔG is drawn against T, ΔH and ΔS can be calculated.[20] Values of ΔG at different temperatures are given in Table 2. The values of ΔH and ΔS for this process were calculated as +15.559 kJ·mol^{-1} and +0.0691 kJ·(mol·K)$^{-1}$, respectively.

As ΔG has negative values, it can be said that the adsorption will occur spontaneously. Conversely, positive ΔH values may

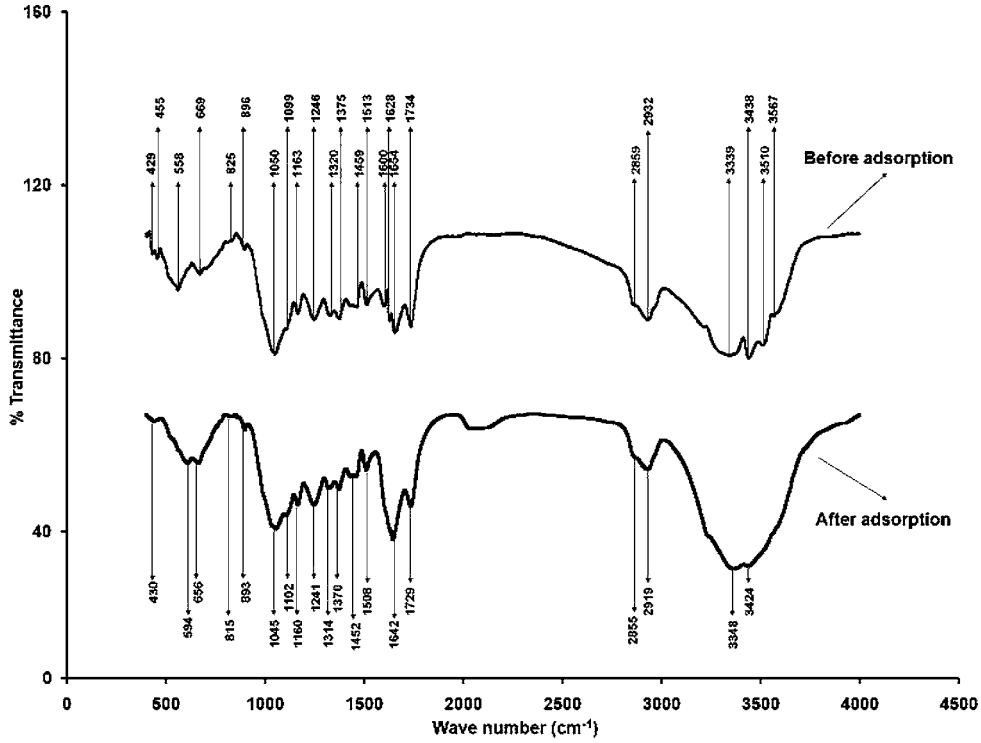

Figure 6. FTIR spectra of rose residue before and after adsorption.

Table 3. FTIR Spectral Characteristics of the Rose Residue before and after Adsorption

IR peak	frequency (cm^{-1}) before ads.	after ads.	differences	assignment
1	3567	disappeared		bonded —OH groups
2	3510	disappeared		bonded —OH groups
3	3438	3424	−14	bonded —OH groups
4	3339	3348	+9	bonded —OH groups
5	2932	2919	−13	aliphatic C—H group
6	2859	2855	−4	aliphatic C—H group
7	1734	1729	−5	C═O stretching
8	1654	1642	−12	C═O stretching
9	1628	disappeared		C═O stretching
10	1600	disappeared		secondary amine group
11	1513	1508	−5	secondary amine group
12	1459	1452	−7	symmetric bending of CH_3
13	1375	1370	−5	symmetric bending of CH_3
14	1320	1314	−6	symmetric bending of CH_3
15	1246	1241	−5	—SO_3 stretching
16	1163	1160	−3	C—O stretching of ether groups
17	1099	1102	+3	C—O stretching of ether groups
18	1050	1045	−5	C—O stretching of ether groups
19	896	893	−3	aromatic —CH stretching
20	825	815	−10	aromatic —CH stretching
21	669	656	−13	—CN stretching
22	558	594	+36	—C—C— group
23	455	430	−25	amine groups
24	429	disappeared		amine groups

suggest that adsorption has an endothermic character and that efficiency will increase as the temperature increases. In light of the above data, it can be said that adsorption has a chemical character.

3.8. FTIR Analysis of the Rose Residue. It is possible to find functional groups that exist in an organic molecule by Fourier transform infrared (FTIR) spectroscopy. An FTIR spectrometer, which uses infrared light, can detect the vibration of functional groups and therefore determine the presence of those functional groups in molecules. It works on the principle of emitting a wide spectrum of IR light toward an organic molecule. Some part of the energy of this light is adsorbed by the molecule through which it passes, and the change in the spectrum is then determined. These increases and decreases in the spectrum of the reflected light are recorded as the IR spectra.[21−23] FTIR images were obtained using a Perkin-Elmer spectrometer.

For determining the functional groups that play a role in removing gallium using the rose residue, the FTIR spectra were measured before and after adsorption. The increases and especially decreases after the adsorption were perceived as an indication that these active groups took part in the adsorption. Of these, the most noteworthy are the disappearing groups.

In Figure 6, there are 24 adsorption bands showing the complex structure of the biosorbent. These are the complex adsorption band characteristics of rose residue. In Table 3, there are 21 bands that show decreases in functional groups. This shows that almost all bands participated in the adsorption. It can be said that only three of these bands did not participate in the adsorption. When analyses of gallium before and after adsorption were performed, the effective groups were bonded OH groups, aliphatic C—H groups, C═O stretching, secondary amine groups, symmetric bending of CH_3, —SO_3 stretching, CO stretching of ether groups, aromatic CH stretching, —CN

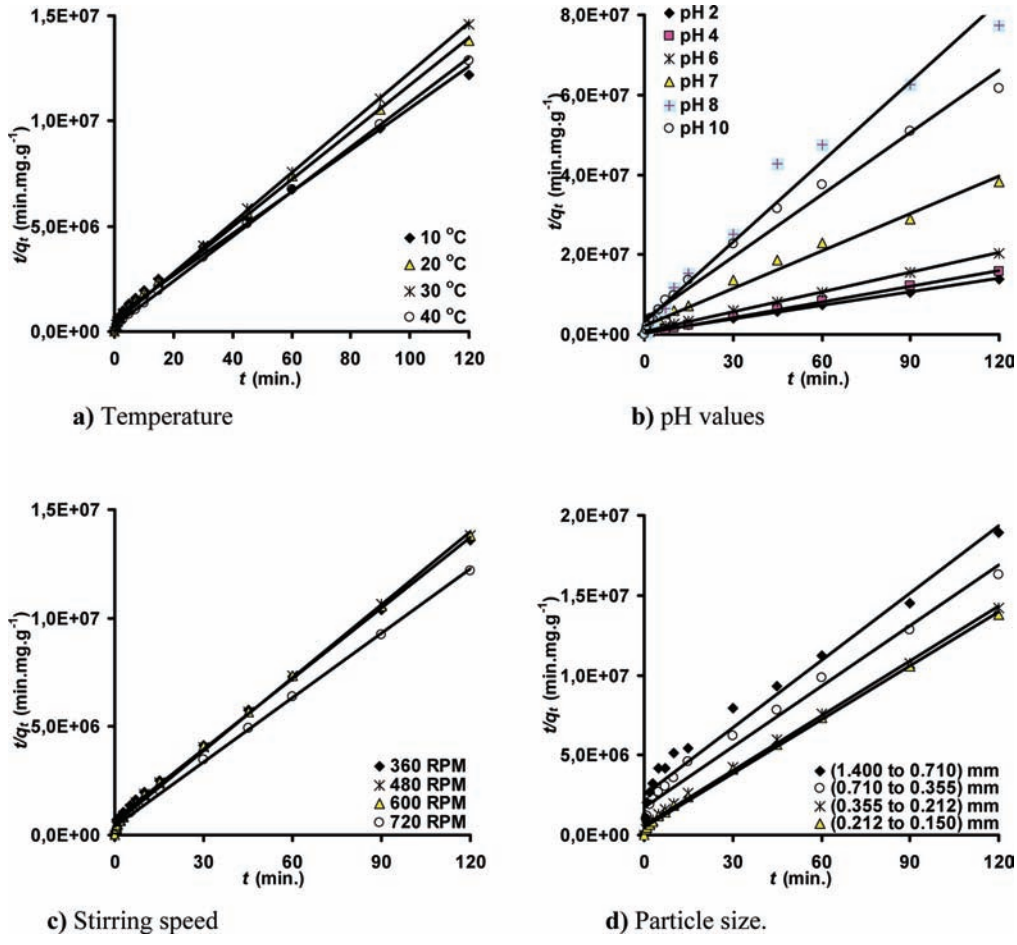

Figure 7. Agreement of experimental data with the pseudo second-order kinetic model.

Table 4. Fit of Experimental Data with the Pseudo Second-Order Kinetic Model for Experimental Parameters

parameters		$q_{e,exp}\cdot10^6$	k	$h\cdot10^6$	R^2	$q_{e,thr}\cdot10^6$
temp., °C	10	9.829	14338.9	1.4563	0.993[a]	10.078
	20	8.693	24857.8	1.9728	0.997[a]	8.9087
	30	8.233	35292.7	2.4984	0.999[a]	8.4138
	40	9.314	44673.1	3.9477	0.999[a]	9.4005
pH	2	8.693	24857.8	1.9728	0.997[a]	8.9087
	4	7.7586	58036.4	3.3451	0.999[a]	7.5920
	6	5.878	38567.9	1.4130	0.998[a]	6.0530
	7	3.145	49125.5	0.5	0.984[a]	3.1903
	8	1.551	148941.4	0.3333	0.981[a]	1.4960
	10	1.946	67542.2	0.25	0.978[a]	1.9239
stirring speed, rpm	360	8.828	16840.2	1.4292	0.996[a]	9.2125
	480	8.687	23751.6	1.8836	0.998[a]	8.9053
	600	8.693	24857.8	1.9728	0.997[a]	8.9087
	720	9.836	24763.7	2.5276	0.998[a]	10.103
particle size, mm	1.400 to 0.710	6.332	6552.7	0.3333	0.960[a]	7.1323
	0.710 to 0.355	7.367	7970.5	0.5	0.976[a]	7.9203
	0.355 to 0.212	8.457	22347	1.7018	0.996[a]	8.7266
	0.212 to 0.150	8.693	24857.8	1.9728	0.997[a]	8.9087

[a] Correlation is significant at the 0.01 level (two-tailed).

stretching, and amine groups, respectively. These groups were very efficient in adsorption in the sense that the process happened very quickly when these groups were involved. In 120 min at pH 2, 87.1 % of ^{67}Ga was absorbed onto the rose residue. As there were no other significant changes, it was thought that the adsorption stabilized and the process ceased at this point. These results indicate the perfect bonding of metal ions with this adsorbent.

3.9. Adsorption Kinetics. Adsorption kinetic models are related to the removal rate of the adsorbent. These models are important in planning the recovery processes with adsorption. There are three main reaction models: reversible first-order, pseudo first-order, and pseudo second-order models.

The graphics concerning the parameters that affect adsorption are given in Figure 7. When these parameters were studied, it was seen that adsorption occurred very quickly and that all of the parameters were active. The kinetic models were tested, and it was found that the process fit the pseudo second-order kinetic model given below.

$$(dq_t/dt) = k(q - q_t)^2 \tag{9}$$

Integration and rearrangement of this equation between the boundary conditions gives the following relation:

$$(t/q_t) = 1/(kq^2) + (1/q)t \tag{10}$$

$$h = kq^2 \tag{11}$$

where h is the initial adsorption rate, t is the adsorption period (min), and k is the kinetic rate constant. A plot of t versus t/q_t should give a straight line if the process fits the pseudo second-order rate model.[24−26]

The calculated data are shown in Table 4. The coefficients of determination of the fits are greater than 0.96. When the regression coefficients were analyzed, it was observed that they were very high. These high coefficients of determination demonstrate that there is a highly significant linear relationship between t and t/q_t in the adsorption of ^{67}Ga. It can be seen in Table 4 that there is little difference between the experimental data and the calculated theoretical values.

3.10. Activation Energy. The value of the activation energy in the Arrhenius equation can give an indication whether the process is physical or chemical. A graph of ln k values of the pseudo second-order rate constant in Table 4 constant versus $1/T$ gives the graph in Figure 8.[26]

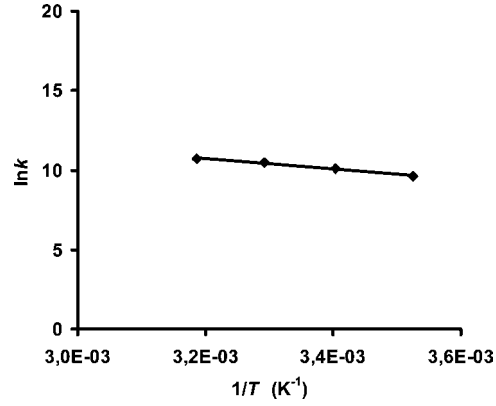

Figure 8. Plot of ln K versus $1/T$.

$$\ln k = \ln A - \frac{E_a}{R}\frac{1}{T} \tag{12}$$

where E_a is the adsorption free energy (J·mol^{-1}) and A is the activation energy. In Figure 8, it can easily be seen that the activation energy is 27.927 kJ·mol^{-1}. A high activation energy also supports chemical adsorption.

3.11. Adsorption Mechanism Study. There are three main transition steps in an adsorption process. These are film diffusion, intraparticular or pore diffusion, and sorption into the inner layer. Generally, the last step is not taken into consideration, because it is regarded as quicker than the other steps. The process is controlled by slower diffusion between film

Table 5. Calculations of the Intraparticle Model

parameters		$t_{1/2}$	$k_i\cdot10^8$	$D\cdot10^{13}$	R^2
temp., °C	10	6.92	10	5.918	0.9316[a]
	20	4.52	9	9.069	0.8745[a]
	30	3.37	8	12.160	0.8089[a]
	40	2.38	8	17.206	0.7746[a]
pH	2	4.52	9	9.069	0.8745[a]
	4	2.27	5	18.044	0.8735[a]
	6	4.28	6	9.560	0.8467[a]
	7	6.38	3	6.418	0.9581[a]
	8	4.49	1	9.125	0.8688[a]
	10	7.70	2	5.321	0.9616[a]

[a] Correlation is significant at the 0.01 level (two-tailed).

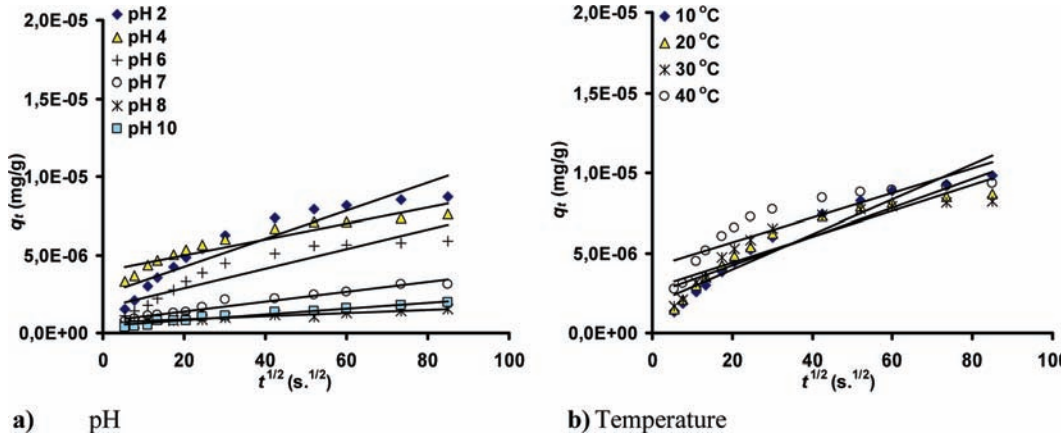

Figure 9. Plots of q_e versus $t_{1/2}$ for different temperature and pH values.

diffusion and pore diffusion.[27] According to Weber et al.,[28] if the retention rate is controlled by the intraparticular diffusion, the amount of the adsorbed material (q_t) changes with the square root of time. So, the adsorption rate is calculated by means of determining adsorption capacity of the adsorbent. The mathematical dependence of q_t versus $t^{0.5}$ is obtained if the sorption process is considered to be influenced by diffusion in the spherical particles and convective diffusion in the solution. The root time dependence, known also as a Weber−Morris plot, may be expressed as follows:[26]

$$q_t = k_i\sqrt{t} + Z \tag{13}$$

The diffusion ratio depends on the surface features of the adsorbent and may be calculated from the following equation;[29,30]

$$f\left(\frac{q_t}{q_e}\right) = -\log\left[1 - \left(\frac{q_t}{q_e}\right)^2\right] = \frac{\pi^2 Dt}{2.3r^2} \tag{14}$$

The half time for the adsorption can be calculated from the following equation for a process with the kinetics of the pseudo second-order rate model;

$$t_{1/2} = \frac{1}{k \cdot q_e} \tag{15}$$

Finally, for the half time period of the process, the following equation for the diffusion coefficient is obtained from eq 15[26]

$$D = \frac{0.030r^2}{t_{1/2}} \tag{16}$$

where k_i is the intraparticular diffusion coefficient ($mg \cdot g^{-1} \cdot s^{-1/2}$), D is the diffusion coefficient ($cm^2 \cdot s^{-1}$), r is the radius of the absorbent particle (cm), and $t_{1/2}$ is the half life (s). In addition to a high correlation ratio, there is a linear relation between $t^{1/2}$ and q_t in Table 5 and Figure 9 ($p < 0.01$). As the adsorption corresponds with the intraparticular diffusion model, it is possible to consider that a pore diffusion mechanism occurs. Looking at the data, the increase of the diffusion coefficient with increasing temperature is an expected behavior. Since increased diffusion with the increase in temperature results in the increased activity of the metal to be adsorbed, the increase in the amount of the material that can hold onto the surface of the metal supports the event described. But the change of the diffusion coefficient with pH is a complicated behavior since the Ga component changes with pH, and therefore every component can have its diffusion value. This effect can be explained by that gallium ions become free of the hydroxide ions with decreasing pH; this can cause the gallium ions to move more easily in the medium.

4. Conclusions

In this study, Ga-67 was adsorbed from liquid wastes by using a biosorbent. Rose residue was used as the biosorbent, and the following results were obtained.

The rose residue had very promising results as an adsorbent. Adsorption was stabilized in 120 min, and the adsorption rate was high. The most effective parameters were the pH, temperature, the particle size, and the adsorbent ratio. For maximum yield of the adsorption, the conditions were determined as 720 rpm for the stirring speed, (0.15 to 0.212) mm for the particle size, 40 °C for the temperature, 2 for the pH, and 15 $g \cdot L^{-1}$ for solid-to-liquid ratio. At the temperature of 40 °C and the solid-to-liquid ratio of 15 $g \cdot L^{-1}$, 99.1 % of Ga-67 was adsorbed. However, lower stirring speed and lower temperature values can be preferred due to economic reasons. For this case, if the parameters were chosen for the stirring speed as 600 rpm, the nominal particle size as (0.15 to 0.212) mm, the temperature as 20 °C, pH as 2, and the solid-to-liquid ratio as 10 $g \cdot L^{-1}$, 87.1 % of Ga-67 was adsorbed. Adsorption was characterized as endothermic, multilayered, heterogeneous, and chemical. The experimental data exhibited good agreement with the isotherm models of Freundlich, Halsey, Henderson, and Smith. Standard Gibbs energy ΔG and ΔH parameters were taken into account, and bioadsorption is believed to have an endothermic character and to be natural. The kinetics of adsorption were seen to fit a pseudosecond-order reaction model. The mechanism of adsorption was believed to be either the pore diffusion or the intraparticle diffusion.

Removing radioactive materials using adsorption is believed to protect the environment from the harmful effects of radiation. Since a radioactive material also turns into a harmful metal in stable states, additional protection from this harmful effect is needed. Elimination of this heavy metal or its radioactive state, which is dumped in the environment, by using adsorbents or storing in lead tanks, seems economically not possible. It is clearly seen that 99.6 % of Ga-67 in 1 m^3 of liquid waste can be adsorbed by using 1.5 kg of an adsorbent. Optimum conditions can be established by analyzing this absorbent among other adsorbents. It is believed that important economical benefits will be gained since the adsorbent, which is a waste matter itself, and the materials it adsorbs will not be dumped into the environment in their harmful form, and they can be recycled with further suitable processes.

Literature Cited

(1) Görpe, A.; Cantez, S. *Pratik Nükleer Tıp;*, İstanbul Tıp Fakültesi Vakfı: İstanbul, 2000.
(2) Kowalsky, R. J.; Perry, J. R. Radiopharmaceuticals in Nuclear Medicine Practice, Appleton & Lange: Norwalk, CT, 1987.
(3) Dean, J. G.; Bosqui, F. L.; Lanoutte, K. H. Removing heavy metals from waste waters. *Environ. Sci. Technol.* **1972**, *6*, 518–524.
(4) Volesky, B. *Bio-sorption and Bio-sorbents. Bio-sorption of Heavy Metals*; CRC Press: Boca Raton, FL, 1990.
(5) Luef, E.; Thedor, P.; Christian, P. K. Adsorbtion of zinc by fungal mycelial wastes. *Appl. Microbiol Biotechnol.* **1991**, *34*, 688–692.
(6) McLean, R. J. C.; Campbell, A. M.; Khu, P. T.; Persaud, A. T.; Bickerton, L. E.; Chemin, D. Repeated use of *Bacillus subtilis* cell walls for copper binding. *J. Microbiol. Biotechnol.* **1994**, *10*, 472–474.
(7) Volesky, B.; Holan, Z. R. Adsorbtion of heavy metals. *Biotechnol. Prog.* **1995**, *11*, 235–250.
(8) Volesky, B.; May-Philips, H. A. Adsorption of heavy metals by *Saccharomyces cerevisiae*. *Appl. Microbiol. Biotechnol.* **1995**, *42*, 797–806.
(9) Medine, E. İ. *Hasta İyonunun I-131'in Amberlit Anyon Değiştirici Reçine ile Tutulması*; Ege Üniversitesi, Fen Bilimleri Enstitüsü, Nükleer Bilimler Anabilim Dalı: Izmir, 2003.
(10) Koshima, H. Adsorption of Iron(III), Gold(III), Gallium(III), Thallium(III) and Antimony(V) on Amberlite XAD and Chelex 100 resins from hydrochloric acid solution. *Anal. Sci.* **1986**, *2*, 225–260.
(11) Taner, S. T.; Demirel, Z.; Üst, Z. *Medikal Alanda Ortaya Çıkan Cr-51 Atıkları İçin Kullanilabilecek Biyolojik Kökenli Bir Adsorban Teklifi*; Ege Üniversitesi Fen Bilimleri Enstitüsü, Nükleer Bilimler Anabilim Dalı: Izmir, 2003.
(12) Kütahyalı, C. *Mangal Kömüründen Üretilen Aktif Karbon Kullanılarak Uranyumun Selektif Adsorpsiyonunun ve Uygulama Alanlarının İncelenmesi*; Ege Üniversitesi Fen Bilimleri Enstitüsü, Nükleer Bilimler Anabilim Dalı: Izmir, 2002.
(13) Sinha, P. K.; Lal, K. B.; Ahmed, J. Removal of radioiodine from liquid effluents. *Waste Manage.* **1997**, *17*, 33–37.
(14) Eroglu, H.; Yapici, S.; Nuhoglu, C.; Varoglu, E. Biosorption of Ga-67 radionuclides from aqueous solutions onto waste pomace of an olive oil factory. *J. Hazard. Mater.* **2009**, *172*, 729–738.
(15) Jackson, E. G.; Byrne, M. J. Metal Ion Speciation in Blood Plasma: Gallium-67-Citrate and MRJ Contrast Agents. *J. Nucl. Med.* **1996**, *37*, 379–386.
(16) Bansode, R. R.; Losso, J. N.; Marshall, W. E.; Rao, R. M.; Portier, R. J. Adsorption of metals ions by pecan shell-based granual activated carbons. *Bioresour. Technol.* **2003**, *89*, 115–119.
(17) Raj, B.; Raj, A. E.; Madan, P.; Siddaramaiah. Modelling of Moisture Sorption Isotherms of Poly(vinyl alcohol)/Starch Films. *J. Appl. Polym. Sci.* **2003**, *89*, 3874.
(18) Başar, A. C. Applicability of The Various Adsorptions Models of Three Dyes Adsorption onto Actived Carbon Prepared Waste Apricot. *J. Hazard. Mater.* **2006**, *135*, 232.
(19) Liu, Y.; Liu, Y. J. Biosorption isotherms, kinetics and thermodynamics. *Sep. Purif. Technol.* **2008**, *61*, 229.
(20) Karadag, D.; Turan, M.; Akgul, E.; Tok, S.; Faki, A. Adsorption Equilibrium and Kinetics of Reactive Black 5 and Reactive Red 239 in Aqueous Solution onto Surfactant-Modified Zeolite. *J. Chem. Eng. Data* **2007**, *52*, 1615.
(21) Robinson, J. W. *Undergraduate Industrial Analysis*; Marcel Dekker Publishing Company: New York, 1987.
(22) Ingle, J. D.; Crouch, S. R. *Spectrochemical Analysis*; Prentice Hall Inc.: Upper Saddle River, NJ, 1988.
(23) Willard, H. H.; Merritt, L. L.; Dean, J. A.; Settle, F. A. *İnstrumental Methods of Analysis*; Wadsworth Publishing Company: Florence, KY, 1988.
(24) Cordero, B.; Lodeiro, P.; Herrero, R.; De Vicente, M. E. S. Biosorption of Cadmium by *Fucus spiralis* more options. *Environ. Chem.* **2004**, *1*, 180.
(25) Miretzky, P.; Munoz, C.; Carrillo-Chavez, A. Fluoride removal from aqueous solution by Ca-pretreated macrophyte biomass. *Environ. Chem.* **2008**, *5*, 68.
(26) Alkan, M.; Doğan, M.; Turhan, Y.; Demirbaş, Ö.; Turan, P. Adsorption kinetics and mechanism of maxilon blue 5G dye on sepiolite from aqueous solutions. *Chem. Eng. J.* **2008**, *139*, 213–223.
(27) Ho, Y. S.; McKay, G. Sorption of dye from aqueous solution by peat. *Chem. Eng. J.* **1998**, *70*, 115–124.
(28) Weber, W. J.; Morris, J. C.; Sanit, J. Kinetics of adsorbtion on carbon from solution. *Eng. Div.* **1963**, *89*, 31.
(29) Kavitha, D.; Namasivayam, C. Experimental and kinetic studies on methylene blue adsorbtion by coir pith carbon. *Bioresour. Technol.* **2007**, *98*, 14–21.
(30) Wang, B. E.; Hu, Y. Y.; Xie, L.; Peng, K. Biosorption behavior of azo dye by inactive CMC immobilized *Aspergillus fumigatus* beads. *Bioresour. Technol.* **2008**, *99*, 794–800.

Received for review December 1, 2009. Accepted May 29, 2010. The support of Atatürk University for the project BAP-2003/372 is highly appreciated.

JE901015A